Effects of dopants on the band structure of quantum dots: A theoretical and experimental study

Joshua T. Wright[1] and Robert W. Meulenberg[1,2,*]

[1]*Department of Physics and Astronomy, University of Maine, Orono, Maine 04469, USA*

[2]*Laboratory for Surface Science and Technology, University of Maine, Orono, Maine 04469, USA*

In this article, we present a theoretical framework that provides predictable results on band gap modifications due to the addition of dopants into CdSe quantum dots (QDs). A theoretical model is developed that predicts a lowering of the conduction band minimum (CBM) due to hybridization. We then use x-ray absorption spectroscopy (XAS) at the Cd M_3-edge to determine the effects of chemical doping on the conduction band (CB) of the QD. Analysis of the XAS onset energy provides evidence for a lowering of the CBM, with our calculations yielding results comparable to experiment within 0.02 eV for tested materials. Also present in the XAS data is a distinct shift of the Cd M_3-edge peak maximum as a function of particle size, suggesting this peak can be used as a tracer to probe the angular momentum resolved shifts in the CB states due to quantum confinement. Our theoretical model can model a variety of dopants and theoretically predict the shift in the energy levels, and should be generalizable towards predicting similar behavior in other materials.

I. INTRODUCTION

Nanoscience researchers have long been fascinated with perfecting chemical doping strategies in semiconductor quantum dots (QDs) since the initial report of Mn^{2+} doping in ZnS QDs by Bhargava *et al.*[1] Since that time, countless reports have been targeted on novel synthetic techniques for doping QDs,[2–5] as well as detailed studies regarding the effects that chemical dopants have on QD properties.[6–8] Recently, groups have reported methods for making *n*- or *p*-type QDs,[9,10] primarily for improving electrical characteristics of the materials.

Our group has been particularly interested in using nonisoelectronic dopants as a means for improving the electrical properties of QDs. A recent report from our group[11] has suggested that hybridization between next nearest neighbors in doped CdSe QDs may lead to a lowering of the conduction band (CB) minimum and could provide a viable method towards tuning energy levels for improved electrical properties. In this current work, we take a more detailed look into the hybridization calculations and reveal a more rigorous and understandable method to calculate hybridization energies. We observe not only how the dopant affects the band structure but also how the dopant may be used as a variable in determining the largest potential effect a dopant may have on tuning the host band structure. We can use results computed from our generalized theory and compare directly to experimental results on the conduction band minimum (CBM) energy using x-ray spectroscopy. We see great agreement between theory and experiment, and suggest our hybridization model can be used in a predictive manner towards understanding how dopants modify the band structure of QD materials.

II. THEORY

In order to develop a theoretical model to describe the effects of dilute chemical impurities on the electronic structure of QDs, it is necessary to first analyze the interaction between two nearby atoms followed by generalization of this result to a larger scale. From first principles, the time independent Schrödinger equation (TISE) is

$$\hat{H}|\Psi_A\rangle = E|\Psi_A\rangle, \tag{1}$$

$$\hat{H} = \hat{T} + \hat{V} = \frac{-\hbar^2}{2m}\nabla^2 + V. \tag{2}$$

The potential, V, in principle will be comprised of several elements; however, in this simplest case a Coulombic interaction can be assumed. By assuming hydrogeniclike orbitals, the form of the wave functions for any element is well known. It is the energy terms that are of interest, so by operating with $\langle\Psi_{A'}|$, which represents another atom of the same element but displaced an integer set of lattice spacings away, this value becomes a constant. This yields

$$\langle\Psi_{A'}|\hat{H}|\Psi_A\rangle = \bar{E}. \tag{3}$$

We now have an energy for a two atom, single element system. This immediately generalizes to any two atom system as

$$\frac{\langle\Psi_B|\hat{H}|\Psi_A\rangle}{\langle\Psi_B|\Psi_A\rangle} = \bar{E}. \tag{4}$$

In the time independent version, assuming that the system is in equilibrium, the energy is simply a scalar.

This model is expanded by introducing hybrid orbitals of the form

$$|\Psi_h\rangle = a|\Psi_A\rangle + b|\Psi_B\rangle, \tag{5}$$

using a linear combination of the atomic orbitals method of constructing the orbitals. Since Ψ_A is a reference point the Ψ_h will take the displaced form. If the atom is of the same element as Ψ_A, then clearly $b = 0$ as there is no contribution from another atom and thus we have the original equation [Eq. (3)] returned. If there is another atom substitutionally replacing an atom of type A, then the orbitals take this hybridization form with the constraints that both are real and that

$$a^2 + b^2 = 1. \tag{6}$$

We now apply the effects of a hybrid orbital onto the TISE,

$$\langle \Psi_h | \hat{H} | \Psi_A \rangle = (a\langle \Psi_{A'} | + b\langle \Psi_{B'} |)\hat{T}\Psi_A \rangle$$
$$+ (a\langle \Psi_{A'} | + b\langle \Psi_{B'} |)\hat{V} | \Psi_A \rangle. \qquad (7)$$

This reduces to a more useful form in

$$\langle \Psi_h | \hat{H} | \Psi_A \rangle = a(\langle \Psi_{A'} | \hat{T} | \Psi_A \rangle + \langle \Psi_{A'} | \hat{V} | \Psi_A \rangle)$$
$$+ b(\langle \Psi_{B'} | \hat{T} | \Psi_A \rangle + \langle \Psi_{B'} | \hat{V} | \Psi_A \rangle). \qquad (8)$$

This integral results in a scaled $a\bar{E}$ and a correction term due to the hybridization effect. In order to fully realize this model for a specific system the V term must be appropriately defined. Assuming the interaction to be Coulombic in nature, it therefore depends on the relative differences in electronegativity such that

$$V = \frac{\alpha \Delta \chi}{r}. \qquad (9)$$

The electronegativity is a unitless value, however, and therefore requires the inclusion of the α term to account for the energy difference. This potential is zero for A interacting with A, which will be useful later when extending this model into the QD region as this will yield a result much like an infinite square well. The hybridization correction is a perturbative addition that affects the overall energy. We wish for α to be element specific and by allowing bond lengths to change it must be radially dependent. This can be modeled very simply as

$$\alpha = \mu C \tau \, d(R), \qquad (10)$$

wherein μ is the chemical potential, C is the concentration of the dopant, τ is the volume of the QD, and $d(R)$ is the radial variation in bond length due to particle size over which the hybridization occurs. This variation of the bond length (in Å) takes the form of

$$d(R) = d_o - \frac{B}{R^2}, \qquad (11)$$

where d_o is the unmodified bond length of the bulk material and B is a fitting parameter that depends on experimental values. Experimentally, it has been shown that for CdSe $d_o = 2.63$ Å and $B = 1.61$.[12] This bond length contraction is purely a result of the size of the QD inducing strain and not due to doping. The low amounts of dopants used do not greatly impact the bond length and so we do not consider them. The modification to the bond lengths can be found either experimentally or theoretically. To further expand the usefulness of this model, we take a functional form of μ such that

$$\mu = D(E) f(E), \qquad (12)$$

where $D(E)$ is a density of states function, thus allowing for more tightly bound orbitals to take a lesser effect on the overall hybridization, and $f(E)$ is an occupation function determining the population of the bands. This combined term, α, is effectively a constant with regards to the potential correction term V as it contains element specific information and is particle size dependent and therefore does not affect the form of the wave functions.

This yields

$$\langle \Psi_h | \hat{H} | \Psi_A \rangle$$
$$= a\bar{E} + b\left(E_k + D(E)f(E)Cd(R)\tau \langle \Psi_B | \frac{\Delta \chi}{r} | \Psi_A \rangle \right), \qquad (13)$$

where we leave the kinetic energy term as E_k for simplicity.

Now that atomic interactions have been modeled, the theory must be adjusted to account for a QD system. A well known crystal structure for CdSe is chosen to determine geometric constraints as well as the nature of the elements in the equation. The zinc blende (ZB) structure limits the equation to four nearest neighbors and 12 next nearest neighbors. Dopants shall be considered as the reference atom as reports[13] indicate that a dopant substitutionally replaces Cd atoms in the lattice, thus resulting in maintaining the original geometry. Cations and anions are topologically identical in the ZB system allowing for simplification via symmetry. Copper is known to act as a d^{10} metal and therefore solutions to the hybridization corrected TISE closely resemble those of Cd with the free electron difference being small in comparison; we, therefore, can approximate the Cu-Se interaction as equal to Cd-Se interaction. Solutions here with nearest neighbor interactions, assuming no other interactions, yield a standard quantum confinement type energy shift based solely on particle size. The free electron in the $4s$ state of Cu is spin coupled to the $5s$ CB minimum of CdSe causing interactions. Since the Cu-Se interaction is defined to be similar to the Cd-Se interaction, effects on next nearest neighbors must be included in order to find perturbations to the overall energy. This results in two perturbative terms:

$$\langle \Psi_h | \hat{H} | \Psi_A \rangle = \bar{E} + \langle \Psi_B | \hat{T} | \Psi_A \rangle + \langle \Psi_B | \hat{V} | \Psi_A \rangle. \qquad (14)$$

The kinetic correction yields a zero sum over the long range and therefore contributes nothing; however, the potential term is the term of interest. Using the well known wave functions for both copper and cadmium we get

$$E_h = \alpha \langle R_{Cu} | \frac{\Delta \chi}{r} | R_{Cd} \rangle = \alpha(-0.0116). \qquad (15)$$

The value for the integral is fixed by the determination of specific wave functions; however, this is for a single Cu-Cd interaction. It is noteworthy that the value is negative; this implies a lowering of the energy, as we would expect from hybridization. We now must consider the interaction between all Cd neighbors:

$$E_h = \sum_i^N \alpha \langle R_{Cu} | \frac{\Delta \chi}{r} | R_{Cd_i} \rangle. \qquad (16)$$

Since the integral is fixed, by symmetry this reduces to six separate equations all with the same value; therefore, we obtain

$$E_h = (-0.0697)\alpha. \qquad (17)$$

Equation (17) represents a rather simple, and elegant, correction term that will depend entirely on the particle size and dopant material.

It is unlikely, however, that only a single dopant enters the QD on average and therefore consideration of multiple

lattice points or larger effects is necessary. This additional consideration results in adjusting Eq. (17) into a summation over each lattice site wherein a dopant atom exists:

$$E_h = \sum_j^M (-0.0697)\alpha_j. \tag{18}$$

Now let us consider next next nearest neighbor interactions. These are again the interactions with Se atoms; however, due to the very long distances involved, the results are three orders of magnitude smaller than those of next nearest neighbors. Therefore, the summation need not be done for N dopants simultaneously, only assume symmetric crystal structure around each dopant and multiply by the number of dopants present. This gives us a more complete view of the α term,

$$\alpha = \mu C d(R), \tag{19}$$

where the term C is a relative doping term. To gain an average value for doping, as sample sizes are on the order of 10^{20} QDs, a ratio of dopants to cadmium describes the relative doping concentration. This value is obtained experimentally using energy dispersive x-ray spectroscopy. In theory, we assume the CdSe system is in a 1:1 atomic ratio for symmetry and simplicity, although it has been shown the stoichiometry of CdSe QDs is not quite 1:1.[14,15] Using the known particle sizes and packing fractions, we can obtain the number of Cd atoms present in the QD to obtain an expression for C in terms of measured values:

$$C = \frac{N_{\text{dopants}}}{N_{\text{Cd}}}. \tag{20}$$

These factors can be combined to demonstrate the change in the energy landscape of CdSe QDs. A parametric plot of energy vs radius vs doping concentration (Fig. 1) exhibits the expected $\frac{1}{R^2}$ dependence from confinement throughout all concentration levels and provides a way of analyzing multiple facets of the relevant phenomena simultaneously.

Inspecting Fig. 1, we can predict a number of interesting aspects of the Cu doped CdSe QD system. For zero doping ($x = 0$, far right), the confinement term is the only modification to the total energy and always remains above the plane
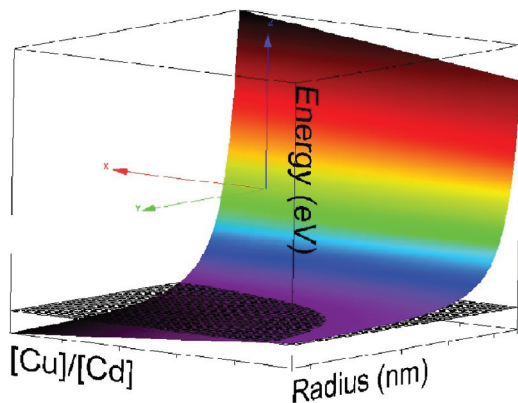
representing the bulk band gap energy. For a given radius ($y = y_0$), the addition of dopants (increasing x) can cause the energy onset [$z(x, y)$] to fall below that of bulk. For instances when the radius is small ($y \to 0$), the energy is always larger than the bulk value, irrespective of dopant concentration. As the particle radius increases, we observe points of particle radii and dopant concentration that cause the energy to fall lower than the bulk band gap energy. The intersection of the theoretical model and the plane demonstrates the points at which the hybridization energy matches the confinement energy. This model provides predictability for material synthesis to obtain specific band gap energies.

III. EXPERIMENT

A. Quantum dot synthesis

The Cu doped CdSe QDs are synthesized using a previously established method.[13] To achieve consistent particle sizes for both doped and undoped materials, a parallel plate methodology was employed in which sample vials were heated simultaneously on a stainless steel block. To perform the synthesis, $\sim$1.2 g of a cadmium selenide thiolate cluster $[Cd_{10}Se_4(SC_6H_5)_{16}](NMe_4)_4$ was mixed with varying amounts of a copper thiolate cluster $[Cu_4(SC_6H_5)_6](NMe_4)_2$ and heated between 240 and 270 °C in $\sim$30 g of hexadecylamine. It should be noted that recent literature has suggested that this synthetic method can produce an alloyed material (CdS_xSe_{1-x}).[16] Typically, the samples present between 1% and 3% sulfur content. As we cannot distinguish between residual sulfur unincorporated into the QD and any sulfur in the QD, any effect due to sulfur is just considered a constant offset for all the samples and will be ignored in our analysis. For all intents and purposes, in this article, we will just refer to the studied particles as "CdSe" QDs.

Determination of the molar percent of Cu in the QDs is performed using energy-dispersive x-ray spectroscopy (EDS). EDS measurements were performed using a Zeiss N-Vision 40 with EDAX attachment. Prior to the EDS measurements, the QDs were rinsed in pyridine 2X to remove adventitious copper species. The measured concentrations varied between 1% and 5% from sample to sample and are summarized in Table I. The QD size and crystallinity are established using

FIG. 1. (Color online) Energy (z) vs particle radius (y) vs doping concentration (x) for Cu doped CdSe QDs. The plane represents the bulk CdSe band gap energy.

TABLE I. Comparison of theoretical $E_{\text{onset}}^{\text{theory}}$ and experimental $E_{\text{onset}}^{\text{expt}}$ (eV) shifts of the CB minimum for Cu doped CdSe QDs. The $\frac{[\text{Cu}]}{[\text{Cd}]}$ term is a relative doping percentage.

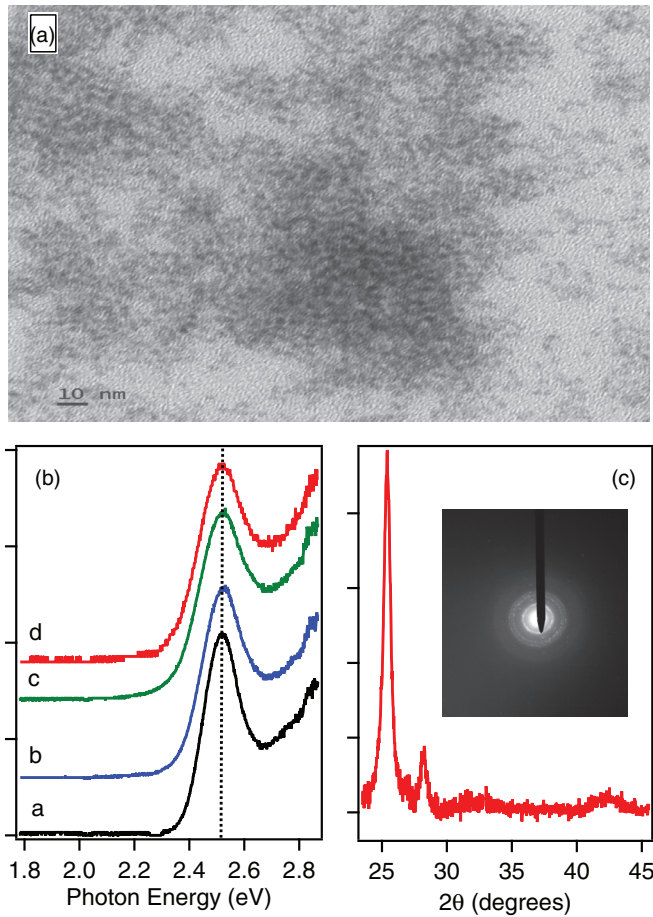| Diameter (Å)	[Cu]/[Cd]	$E_{\text{onset}}^{\text{theory}}$ (eV)	$E_{\text{onset}}^{\text{expt}}$ (eV)
20	n/a	0.59	0.6
20	1.14	0.39	0.4
20	1.24	0.37	0.4
20	1.79	0.27	0.3
20	2.21	0.21	0.2
30	n/a	0.26	0.3
30	1.3	0.01	0.1
30	1.68	−0.07	−0.1
30	3.53	−0.43	−0.4
30	4.46	−0.61	−0.6

FIG. 2. (Color online) (a) TEM image (100 kV) of 1.68% Cu doped 30 Å CdSe QDs. (b) UV-visible spectra for (*a*) undoped, (*b*) 1.79%, (*c*) 1.24%, and (*d*) 2.21% doped Cu CdSe QDs, and (c) XRD spectrum for 1.68% Cu doped 30 Å CdSe QD. The peak ∼38° is due to the silicon substrate. The inset is a small angle electron diffraction image of the sample in (a) clearly demonstrating ZB structure.

UV-Visible spectroscopy [Fig. 2(b)], transmission electron microscopy (TEM) [Fig. 2(a)], and powder x-ray diffraction (XRD) [Fig. 2(c)]. UV-Visible measurements were taken with an Ocean Optics USB-2000+ CCD spectrometer, TEM measurements were performed using a Philips/FEI CM10, and XRD measurements were performed on a PANalytical X'PertPro diffractometer with Cu $K\alpha$ radiation. In this study, two different sizes of Cu:CdSe QDs (∼20 and ∼30 Å diameter) have been prepared and compared. We note that we have also prepared 45 Å QDs, but as we were unable to perform a full series of x-ray absorption measurements on them, that data cannot be used for comparison purposes. We were able to use these particles for optical measurements.

One important note is to point out the exciton absorption peak at ∼2.5 eV [Fig. 2(b)] remains fixed as the doping concentration increases providing the size invariance need for comparison to our theoretical model. This size invariance as a function of doping concentration is observed for all the synthesized samples in this study. TEM and XRD show well formed crystalline materials with the zinc blende crystal structure. Our TEM analysis in Fig. 2(a) shows an average QD size of 27.8 ± 1.5 Å showing narrow size dispersities in our materials.

B. Soft x-ray spectroscopy

The electronic structure of these materials was probed using soft x-ray absorption spectroscopy (XAS) on the PGM beamline at the Laboratorio Nacional de Luz Sincrotron (LNLS), located at CNPEM in Campinas, Brazil. The pyridine coated Cu:CdSe QD samples were dispersed in a small amount of hexane and allowed to slowly evaporate on a Si wafer. These samples were mounted onto carbon tape and introduced in an ultrahigh vacuum chamber with base pressure on the order of 10^{-7} Torr. XAS measurements were conducted using the total electron yield (TEY) detection method. With the TEY method, the total photocurrent into the sample is measured as the photon energy is scanned through the absorption edges. The current from a highly transmissive gold grid, I_0, located upstream on the beamline was used to normalize the XAS spectra. The experimental energy resolution was ∼25 meV at the Cd M_3-edge. Some of the data presented in this article was collected at the Canadian Light Source (CLS) as previously described.[11]

IV. RESULTS AND DISCUSSION

A. Use of Cd M_3-edge XAS as tracer for quantum dot particle size

Using traditional means of obtaining particle sizes (i.e., see Fig. 2) for the QDs in this manuscript have yielded sizes of 24, 31, and 43 Å. In prior work, however, we suggested that certain features present in XAS may be used to determine particle size.[11] Figure 3 displays Cd M_3-edge XAS for a series of undoped CdSe QDs. It is obvious to the eye that the primary peak energy (at ∼619 eV) shifts for all the plotted spectra. The shifts in this peak (with respect to bulk) are (b) 0.5, (c) 0.8, and (d) 0.9 eV. Comparison of these shifts to the theoretical shifts of the CB minimum[17] yield particle sizes of 45, 29, and 23 Å, respectively. The derived particle sizes from the XAS peak shift agree well with the particle sizes from both optical absorption and TEM which confirms the ability to use this peak as a tracer for QD particle sizes. For the remainder of this article, we will refer to the particle sizes as nominally 20, 30, and 45 Å.

B. Oxidation state of copper dopants

The identification of the oxidation state of Cu dopants in II-VI QDs has been controversial. Both we[13] and others[18] have argued for Cu(I) doping, leading to a d^{10} dopant that is magnetically silent, while other groups have found evidence for Cu(II) doping.[19–21] As Cu(II) is d^9, we expect this paramagnetic ($s = \frac{1}{2}$) center to be magnetically active, and therefore either electron spin resonance or magnetometry should be employed to confirm this oxidation state.[20] It should be noted that optical measurements cannot alone be used to unambiguously determine the differences between Cu(I) and Cu(II) centers in these materials.

Figure 4 displays dc magnetic susceptibility and isothermal magnetization spectra for 1.79% doped 20 Å radius Cu:CdSe. The isothermal magnetization spectrum [Fig. 4(b)] can be fit to a Langevin function with a saturation magnetization, M_s, of 6×10^{-3} emu/g and an effective magnetic moment, μ_{eff}, of $4.9\mu_B$. This value for μ_{eff} agrees well with the spin only
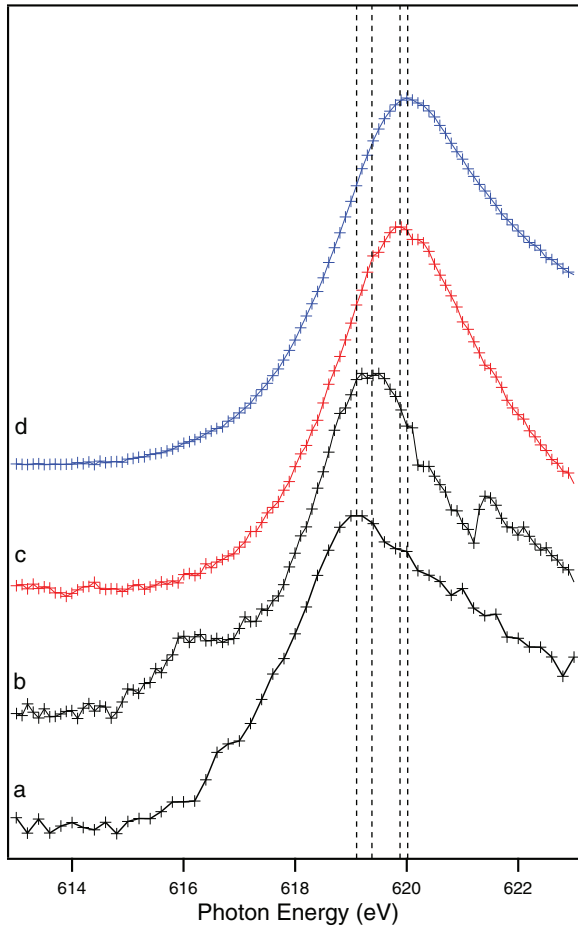
FIG. 3. (Color online) Cd M_3-edge XAS spectra for three sizes (*a*) bulk, (*b*) 45 Å, (*c*) 30 Å, and (*d*) 20 Å of undoped CdSe QDs.

FIG. 4. (Color online) (a) dc magnetic susceptibility ($\mu_o H = 1000$ Oe) and (b) isothermal ($T = 2$ K) magnetization measurements on 1.79% Cu doped 20 Å CdSe QDs. Magnetometery measurements were performed on a Quantum Design MPMS-XL.

value for Fe(II) impurities. The dc magnetic susceptibility spectrum [Fig. 4(a)] can be fit with a Curie-Weiss law through the entire temperature range with a Curie constant, C, of 4.8×10^{-7} (emu K)/g. This derived Curie constant is too small if one considers the magnetization arises solely from an ~2% doped Cu(II) ($s = \frac{1}{2}$) system. Indeed, the value of C is consistent with ~10 ppm of Fe(II) ($s = 2$). Our magnetometry measurements show no evidence for Cu(II) in any of our materials, but cannot confirm the presence of Cu(I).

For verification of the Cu(I) state, we turn to XAS. Here we use the Cu L_3-edge as we have shown that this edge provides a spectroscopic signature for the oxidation state of Cu dopants in QDs.[13] As shown in Fig. 5, the appearance of the feature at ~933 eV, with a minimal peak at ~930 eV, suggests the Cu(I) oxidation state. The XAS and magnetometry measurements, when considered together, provide clear evidence for the Cu(I) oxidation state in our materials.

C. XAS analysis of energy onset

With the oxidation state clearly identified as Cu(I), we wish to now discuss the interplay between chemical doping and particle size on the CB energy of the QDs. We note that the calculations in Sec. II do not change if one considers Cu(I) versus Cu(II), so the hybridization effect is a property of the dopant atom itself, and not necessarily correlated to the native
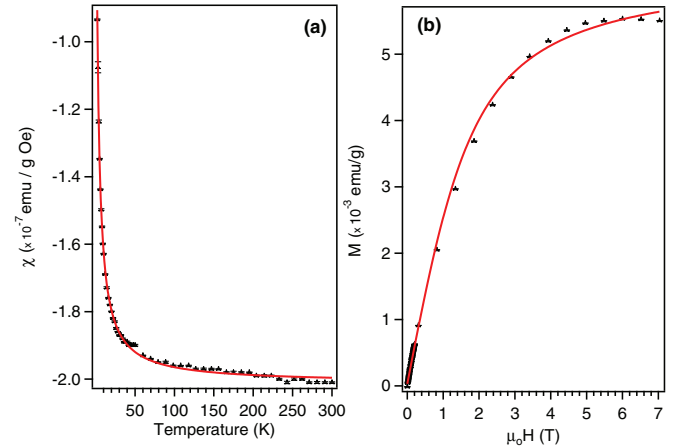
electronic structure of the dopant. Using a previously defined method[11] to determine the experimental value of the onset energy for the CB minimum, the theoretical model, described in Sec. II, should predict the shifts of the band gap due to both the hybridization and confinement terms. By referencing the bulk onset to zero these differences can become more readily seen.

Figure 6(a) displays several key features of the Cd M_3-edge XAS spectra for the 20 Å CdSe QD with varying Cu dopant concentrations. First, we again note that the primary peak is shifted by 0.9 eV for all of the QD samples. As already stated, this shift corresponds to a particle size of $\simeq$20 Å[17] and is verified by optical measurements (Fig. 2). Second, for any doping concentration the energy onset for the QD always remains higher than the corresponding bulk value. This result is matched by theory (Fig. 6), as the hybridization
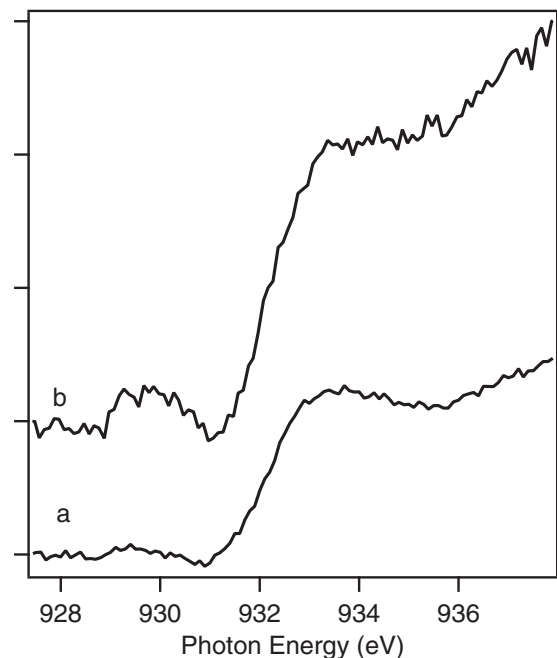

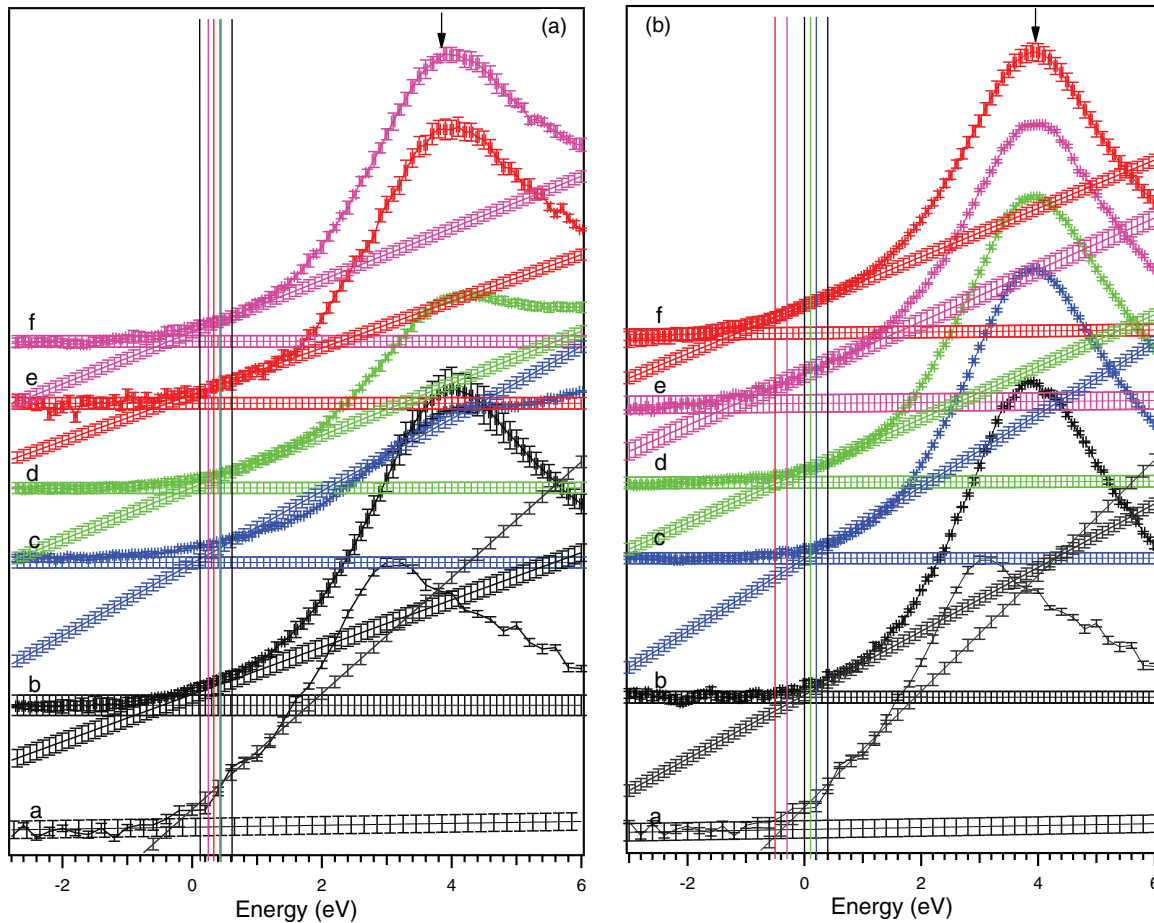FIG. 5. Cu L_3-edge XAS spectra for (*a*) 20 Å 1.79% Cu and (*b*) 30 Å 1.68% Cu doped CdSe QDs.

FIG. 6. (Color online) Cd M_3-edge XAS of (a) 20 Å CdSe QDs as a function of Cu dopant concentration (*a*) bulk, (*b*) undoped, (*c*) 1.14%, (*d*) 1.24%, (*e*) 1.79%, and (*f*) 2.21% and (b) 30 Å CdSe QDs as a function of Cu dopant concentration (*a*) bulk, (*b*) undoped, (*c*) 1.3%, (*d*) 1.68%, (*e*) 3.53%, and (*f*) 4.46%. The baseline and intersection points are marked for the reader to determine the point of the onset.

effect cannot overcome the confinement effect, but is still visible as a shift to lower energy from the undoped sample. When we examine a larger particle size, we observe a shift in the primary peak of 0.8 eV, corresponding to a 3.1 nm particle. More importantly, however, is the appearance of the onset energy occurring at energies lower than the bulk onset energy for high dopant concentrations. It is readily apparent that a large amount of dopant, present in two of the samples, can cause a hybridization effect strong enough to overcome quantum confinement. Comparison to our theoretical model (Fig. 1) accurately reproduces these shifts. The comparison between the experimental and theoretical onset energies are summarized in Table I. When compared to previously published data on a larger QD size,[11] we find that hybridization effects occur at much lower doping concentrations and fully support our hybridization model.

D. Impact of hybridization on the optical properties of copper doped CdSe quantum dots

A recent study[19] has suggested that the low energy photoluminescence (PL) observed in Cu doped CdSe QDs can be used as a tool to detect changes in the CB edge energy as a function of particle size. This method depends solely upon the assumption that the Cu d levels are pinned in the gap when the material transitions from bulk to QD. Using these methods, a very nice agreement in CB energy scaling was achieved, comparable to the shifts derived by us using XAS.[17] This method works, in principle, if the CB minimum does not change within a single size range as a function of doping concentration. With our hybridization model, however, the CB minimum energy can be tuned depending on the amount of dopant, suggesting that the Cu related PL is tunable by changing dopant concentration within a constant particle size series.

Figure 7 presents schematic band diagrams for bulk CdSe and 45, 30, and 20 Å CdSe QDs. The bulk CdSe VB energy is set to zero and the CB shifts for the QDs are obtained from our current XAS measurements with the VB shifts coming from prior work.[22] Also included in the figure is the appearance of levels below the native CB minimum occurring from hybridization. In the most basic framework, in the absence of hybridization effects, we would expect the Cu based PL that originates from an electron in the CB and a hole in the Cu d levels to be size dependent and not depend on Cu concentration.[19] Our model, however, predicts a Cu based PL that is not only size dependent but also tunable with dopant concentration.

Figure 8(a) plots 20 Å Cu doped CdSe QDs as a function of dopant concentration. We observe a PL band at ~1.82 eV that does not change with dopant concentration with zero band edge
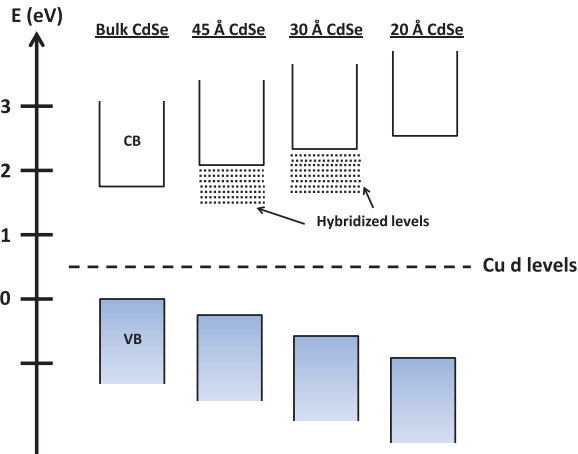
FIG. 7. (Color online) Schematic band diagram for CdSe bulk and QDs illustrating the addition of hybrid states below the CB minimum.

PL. The observation of zero band edge PL is significant. This result again supports the assignment of Cu(I) as the dominant species in our materials. If our QDs contained Cu(II), a hole in the Cu d level would always be present, suggesting that, upon photoexcitation and creation of the exciton in the QD,

there are competing radiative pathways that can lead to both band edge PL and Cu related PL.[19] For Cu(I) doping with a completely filled d shell, the hole must be captured after creation of the exciton via hole transport from the CdSe VB to the Cu d level. This hole transport leads to an optically inactive band edge state and would result in only Cu based PL, as observed experimentally.

For the 30 Å QDs, we observe a PL band at $\sim$1.76 eV for the lowest doped sample, but the PL energy slowly decreases with increasing doping concentration (to a value of $\sim$1.67 eV). The 45 Å QDs also exhibit a Cu concentration dependence in the PL energy, reaching a lowest value of $\sim$1.50 eV for the largest Cu concentration. What these results commonly point to is that the lowest energy emissive state in these materials cannot be assigned solely to the CdSe CB minimum. Indeed, there exists states below the CB minimum that contribute to the Cu based PL, most likely attributable to the hybridized states described in this article (see Fig. 7). We do note, however, there is not quantitative agreement between the observed PL energy and our calculated hybridization energies. We also note that the shifting of the PL as a function of concentration will eventually reach a limit, as there will be a transition from "doping" of Cu to a ternary or "Cd doped" copper selenide material. Indeed, the optical properties are more likely fairly complex and should be studied in further detail.

V. CONCLUSIONS

We have developed a theoretical model that can predict the effects of hybridization induced lowering of conduction band edges in quantum dots. The model matches experimental results (from x-ray absorption measurements) within $\sim$0.02 eV on average. The current model is built upon a previous model by considering a size dependent bond length with the particle size contraction leading to a better prediction on understanding the effects of hybridization on the electronic structure. This model requires no empirical fitting factors and requires only the knowledge of doping levels in a material and the size dependent changes in lattice parameters. The hybridization model can provide some qualitative insight towards understanding the unique optical properties of doped quantum dot systems. Overall, this work suggests that there is still interesting physics to understand about how dopants can affect not only the electronic structure but also the optical properties.
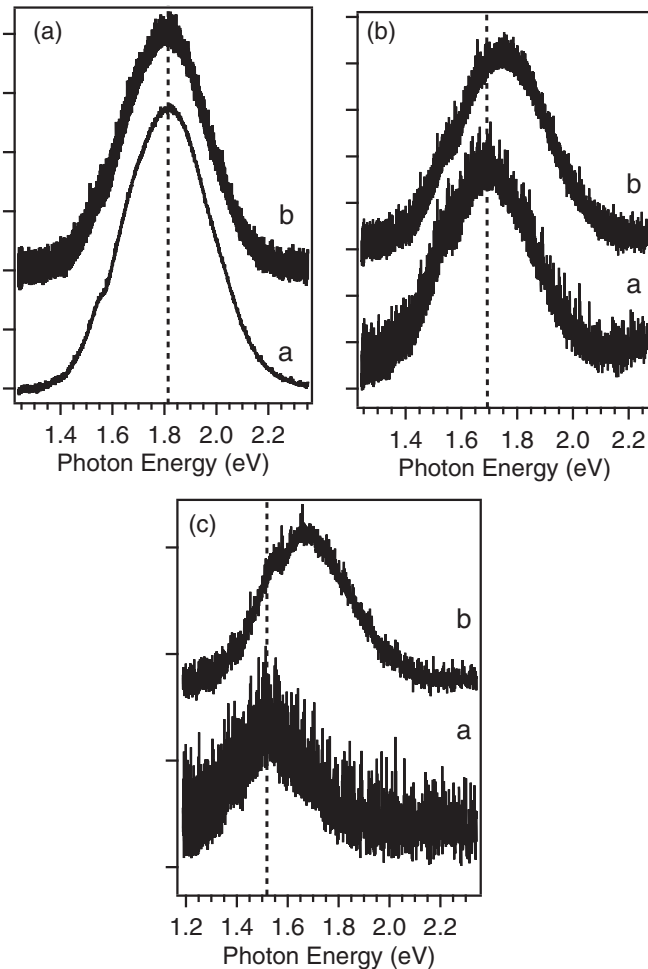

FIG. 8. Photoluminescence spectra (excitation at 3.06 eV) for (a) 23 Å, (b) 31 Å, and (c) 45 Å CdSe QDs with Cu doping levels of (*a*) $\sim$4% and (*b*) $\sim$1%.

*Corresponding author: robert.meulenberg@maine.edu

[1] R. N. Bhargava, D. Gallagher, X. Hong, and A. Nurmikko, Phys. Rev. Lett. **72**, 416 (1994).

[2] F. V. Mikulec, M. Kuno, M. Bennati, D. A. Hall, R. G. Griffin, and M. G. Bawendi, J. Am. Chem. Soc. **122**, 2532 (2000).

[3] D. A. Schwartz, N. S. Norberg, Q. P. Nguyen, J. M. Parker, and D. R. Gamelin, J. Am. Chem. Soc. **125**, 13205 (2003).

[4] S. C. Erwin, L. J. Zu, M. I. Haftel, A. L. Efros, T. A. Kennedy, and D. J. Norris, Nature (London) **436**, 91 (2005).

[5] N. Pradhan and X. G. Peng, J. Am. Chem. Soc. **129**, 3339 (2007).

[6] P. I. Archer, S. A. Santangelo, and D. R. Gamelin, Nano Lett. **7**, 1037 (2007).

[7] R. Beaulac, P. I. Archer, S. T. Ochsenbein, and D. R. Gamelin, Adv. Funct. Mater. **18**, 3873 (2008).

[8] R. G. Xie and X. G. Peng, J. Am. Chem. Soc. **131**, 10645 (2009).

[9] D. Yu, C. J. Wang, and P. Guyot-Sionnest, Science **300**, 1277 (2003).

[10] D. V. Talapin and C. B. Murray, Science **310**, 86 (2005).

[11] J. T. Wright and R. W. Meulenberg, Appl. Phys. Lett. **101**, 193104 (2012).

[12] J. Y. Zhang, X. Y. Wang, M. Xiao, L. Qu, and X. Peng, Appl. Phys. Lett. **81**, 2076 (2002).

[13] R. W. Meulenberg, T. van Buuren, K. M. Hanif, T. M. Willey, G. F. Strouse, and L. J. Terminello, Nano Lett. **4**, 2277 (2004).

[14] J. Taylor, T. Kippeny, and S. J. Rosenthal, J. Cluster Sci. **12**, 571 (2001).

[15] S. W. H. Eijt, A. Van Veen, H. Schut, P. E. Mijnarends, A. B. Denison, B. Barbiellini, and A. Bansil, Nat. Mater. **5**, 23 (2006).

[16] D. D. Lovingood, R. E. Oyler, and G. F. Strouse, J. Am. Chem. Soc. **130**, 17004 (2008).

[17] J. R. I. Lee, R. W. Meulenberg, K. M. Hanif, H. Mattoussi, J. E. Klepeis, L. J. Terminello, and T. van Buuren, Phys. Rev. Lett. **98**, 146803 (2007).

[18] B. B. Srivastava, S. Jana, and N. Pradhan, J. Am. Chem. Soc. **133**, 1007 (2011).

[19] G. K. Grandhi, R. Tomar, and R. Viswanatha, ACS Nano **6**, 9751 (2012).

[20] R. Viswanatha, S. Brovelli, A. Pandey, S. A. Crooker, and V. I. Klimov, Nano Lett. **11**, 4753 (2011).

[21] J. F. Suyver, T. van der Beek, S. F. Wuister, J. J. Kelly, and A. Meijerink, Appl. Phys. Lett. **79**, 4222 (2001).

[22] R. W. Meulenberg, J. R. I. Lee, A. Wolcott, J. Z. Zhang, L. J. Terminello, and T. van Buuren, ACS Nano **3**, 325 (2009).